

Determination of Forming Limit Stress Diagram for Formability Prediction of SPCE 270 Steel Sheet

**Sansot PANICH¹, Vitoon UTHAISANGSUK^{2*}, Jittichai JUNTARATIN³
and Surasak SURANUNTCHAI¹**

¹*Department of Tool and Materials Engineering, Faculty of Engineering, King Mongkut's University of Technology Thonburi, Bangkok 10140*

²*Department of Mechanical Engineering, Faculty of Engineering, King Mongkut's University of Technology Thonburi, Bangkok 10140*

³*Iron and Steel Institute of Thailand,
Soi Trimit, Rama 4 Road, Phrakonong, Klong-toey, Bangkok 10110*

Abstract

The aim of this research is to apply numerical Finite Element Method (FEM) for determining Forming Limit Stress Diagram (FLSD) of sheet steel of grade SPCE 270. As a failure criterion for formability prediction in sheet metal forming process, the conventional Forming Limit Diagram (FLD) is often used. The FLD is a strain based criterion, by which the principal strains at failure are evaluated. Many investigations showed that the FLD is dependent on forming history and strain path. However, the stress based criterion does not confirm this dependency. This criterion is more robust against any changes in the strain path occurring in a forming process. To determine the stress based criterion or the Forming Limit Stress Curve (FLSC), the FLD was initially determined by the Limiting Dome Height (LDH) test. Afterwards, the LDH test was simulated by FEM using the FLD data as a failure criterion. Calculated major and minor stresses were used to construct the FLSC. Finally, an industrial automotive part was taken in order to validate the applicability of the FLD and FLSD criterion. The investigations confirmed that the FLD is insufficient for evaluating parts being manufactured in complex forming process with strain path changes. Nevertheless, the results exhibited that the FLSD is a more precise tool for characterizing formability of steel sheet.

Key words: Forming limit diagram, Forming limit stress diagram, Failure criterion, Formability, FEM, SPCE 270 steel sheet

Introduction

The conventional Forming Limit Diagram (FLD) is a well accepted tool for predicting formability and safety limit of material in sheet metal forming processes. The FLD can be determined using a procedure suggested by the American Society of Testing Materials (ASTM). The standard test method for determining a forming limit curve was published in ASTM E 2218-02. This method is also called the Limit Dome Height (LDH) test that is equipped with a hemispherical punch having a diameter of 100 mm. Hereby, sheet metal specimens with the same width of 200 mm trimmed to various form shapes with a radius of 0, 40, 50, 57.5, 65, 72.5 and 80 mm were used. These different specimen sizes describe different states of stress during forming process. The principal strains φ_1 and φ_2 measured for different sample dimensions

are determined, plotted against each other, and connected to form a curve. This curve, also known as the forming limit curve, represents a strain based failure criterion, which describes the transition from safe material behavior to material failure. The material can sustain the strains underneath the forming limit curve without failure due to necking or fracturing. Generally, the FLDs are based on the assumption of a linear or a quasi-linear strain path ($d\varphi_2/d\varphi_1 \approx \text{const.}$). When analyzing the formability of sheet metals, the question arises to what extent the FLD can be used as a standard of comparison. A FLD for pre-strained materials is influenced by the interactions between different states of stress. In this case, material undergoing pre-deformation ($d\varphi_2/d\varphi_1 \approx \text{const.}$) can show higher or lower forming limit values than material without pre-deformation. For example, the FLD curve will shift

*Corresponding author Tel: +66 2470 9274; Fax: +66 2470 9111; E-mail: vitoon.uth@kmutt.ac.th

to higher ϕ_1 -values if a plane stretch forming ($d\phi_2/d\phi_1 = 1$) is applied after a uniaxial tensile loading ($d\phi_2/d\phi_1 = -1/2$) or after a deep drawing loading ($d\phi_2/d\phi_1 = -1$). On the other hand, if a stretch forming is followed by a deep drawing, the FLD curve will shift to lower ϕ_1 values, as shown in Figure 1(a). Thus, it can be established that the FLD is very sensitive to non-linear strain paths. In industrial application, complex parts are usually manufactured in multi-step forming processes, by which the influence of non-proportional forming history on the FLD can be critical⁽¹¹⁾. Under such conditions, the FLD cannot be used to predict whether this manufacturing method will be successful or fail⁽¹⁾. Additionally, several authors have proved that the FLD is only applicable for a deformation with linear strain ratio^(8-10, 21).

The forming limit stress diagram (FLSD) was first introduced by Arrieux and his co-workers^(1-3, 13). Subsequently, several investigations by Stoughton⁽¹⁵⁻¹⁷⁾ concerned a new failure criterion formulated by the principal stresses. By calculating FLSD, strain hardening and anisotropy of examined material were taken into account under the assumption of the Hill's yield criterion and the flow law according to Levy-Mises. It has been shown that a single forming limit stress curve could be determined from various forming limit diagrams. As a result, the FLSD is less dependent on the forming history and strain path. Thus, it can be used to predict a necking occurrence for any kind of drawn parts undergoing complex strain paths. The failure criterion FLSD exhibits the working range in which a material can be deformed without failure in sheet metal forming process, Figure 1(b). For example, FLSDs calculated by coupling with different yield criteria are demonstrated in Figure 1(c).

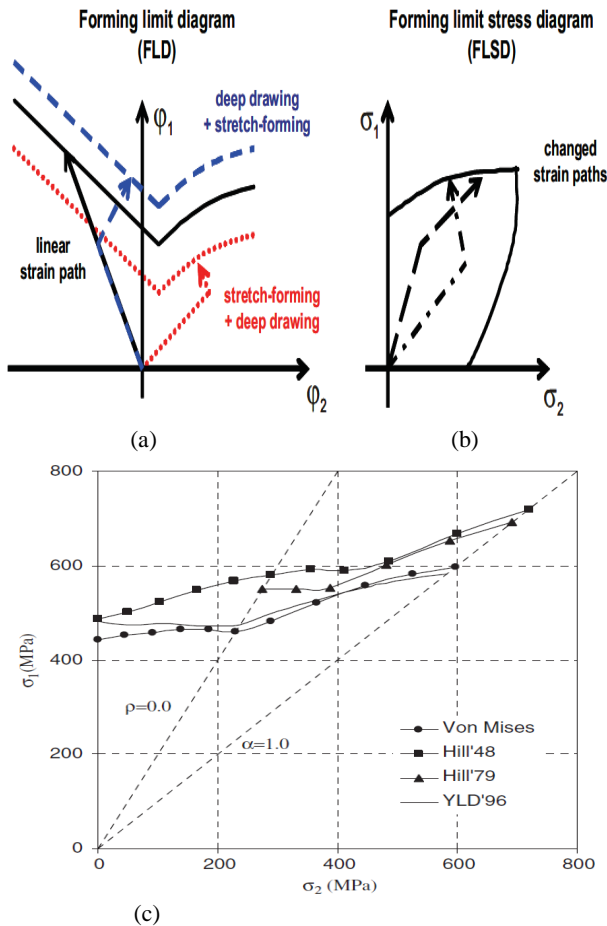


Figure 1. (a) Strain based failure criterion FLD^(18, 20) (b) and stress based failure criterion FLSD^(18, 20), and (c) Forming limit stress diagram of a bake-Hardening Steel (BH steel) coupled with different yield criteria⁽⁷⁾.

The determination of FLSD presented by Arrieux et al.⁽¹⁾ deals with the information obtained from total deformation paths of the crack initiating area. Here, the Nakazima-strip-test was applied to determine the FLD in the first place. Then, stress values must be calculated incrementally according to the Levy-Mises flow law. Another possibility for calculating the stress values during the forming test is the Finite Element Method (FEM)⁽¹⁸⁾. By using FEM, numerically calculated stresses can be evaluated incrementally at the crack-critical area when the FLD failure criterion is reached. The objective of this study is to introduce the stress based FLSD criterion and to show how both FLD and FLSD work. In this work, the FLSD was applied to predict material formability of an automotive part, and the FLSD criterion was compared with the FLD criterion. The investigated part is made of a mild steel sheet SPCE270 that is used as the cover of fuel tank in a vehicle. Numerical simulations of the Limit Dome Height (LDH) testing were performed using the commercial FE program ABAQUS in order to determine the FLSD. Both isotropic and anisotropic Hill's yield criteria are considered in the simulation. Subsequently, the strain based failure criterion FLD and stress based failure criterion FLSD were examined with numerical forming process of that automotive part to verify their ability for predicting the material formability behavior. Additionally, it was found that accuracy of the FLSD criterion depends strongly on the yield function applied.

Materials and Experimental Procedures

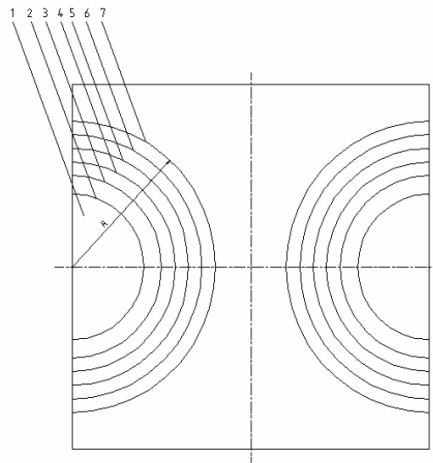
Determination of the Forming Limit Diagram (FLD)

For experimental determination of FLD for the SPCE 270 steel sheet, the limit dome height testing according to the American Society of Testing Materials (ASTM) as published in ASTM E 2218-02 was carried out on an 80-ton hydraulic press machine at room temperature. The used sheet metal samples have the same width and length of

200 mm. They were trimmed with different trim radius varying from 40 up to 80 mm. The sheet specimens have a thickness of 0.8 mm. Figure 2(a) and (b) depict the samples after forming and the used sample dimensions, respectively. The samples were pressed and formed by a hemispherical punch with a diameter of 100 mm until fracture, Figure 2(a). Figure 2(c) shows experimental setup of the LDH tool. Testing for each sample dimension was repeated three times in order to confirm the reproducibility.

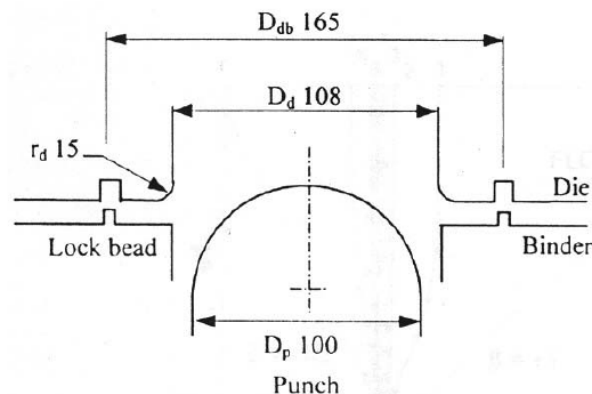


(a)



Position	1	2	3	4	5	6	7
R (mm)	0	40	50	57.5	65	72.5	80

(b)



(c)

Figure 2. Limit dome height test for determining FLD⁽¹⁴⁾ (a) A pressed specimen at fracture after LDH test, (b) specimen geometries, and (c) tool drawing of LDH test.

To obtain major and minor principle strains of the deformed samples, electro-chemical-etching machine was used to generate a 2.5 mm - diameter circular grid pattern on the surface of blank sheet, as shown in Figure 3. The deformations of circular grids in safe, neck and crack locations on the specimens after forming were accurately measured using an image analysis program by microscope. Figure 4 illustrates the cracking and necking area on the samples with a reference pattern. The deformation measurement of the sheet samples was carried out after every entire forming test. The calculated major and minor principle true strains were plotted in a diagram to construct the FLC. The determined FLD for the investigated steel is represented in Figure 5 in form of individual calculated strain values from each sample size after LDH testing and a single fitted forming limit curve. The LDH testing was simulated afterwards in ABAQUS in order to determine the Forming Limit Stress Curve (FLSC). Details of the simulation are discussed in the next chapter.



Figure 3. Circular Grids were marked onto the surface of blank sheet using electrochemical-etching technique ⁽¹⁴⁾.

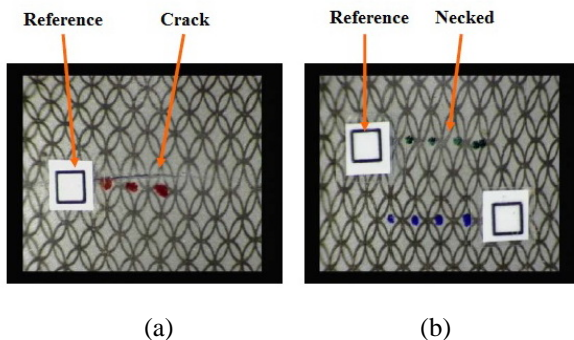


Figure 4. (a) Deformation of circular grids near surface crack. (b) Deformation of circular grids in necked area ⁽¹⁴⁾.

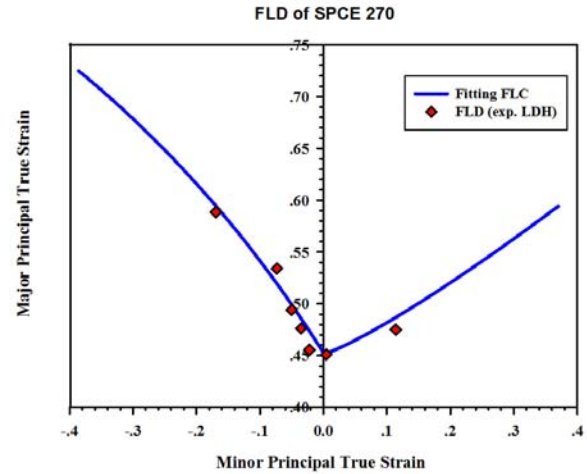


Figure 5. Determined forming limit diagram for SPCE 270 steel sheet.

Determination of Forming Limit Stress Diagram (FLSD)

The determination of the FLSD refers basically to the flow law according to Levy-Mises as given by:

$$d\varepsilon_{ij} = d\lambda s_{ij}(\varepsilon_{ij}) \quad (1)$$

The tensor of incremental strain contribution $d\varepsilon_{ij}$ is calculated during the forming of sheet metal into the appropriate tensor of deviatoric stress s_{ij} , or into the stress tensor σ_{ij} by means of the plastic slip parameter $d\lambda$, which represents the material behavior of all local points in every time interval. This can be done only if the total deformation paths are known for the failure area of the sheet samples from the LDH testing. Therefore, it is not possible to calculate the principal stresses σ_1 and σ_2 directly from the strains ε_1 and ε_2 of the FLD. Otherwise, experimentally determining entire deformation paths during sheet forming process is extremely complex and requires a special measurement system. By means of FEM simulation, strain and stress values can be simultaneously calculated for every interested area on the sheet metal sample and for each loading step. Then, the maximum stresses can be evaluated when the deformation of the crack-critical area of the samples reaches the FLD-failure criterion in the simulation.

To determine the FLSD, the LDH testing was simulated by the commercial FEM program ABAQUS. In this work, 3D shell element was applied for specimens. FE-models of tooling were defined as discrete rigid. The dimension of all FE

model parts were designed to be consistent with the geometries of punch, die and blank holder in the experimental LDH testing. The model for specimens were meshed with elements that were fine enough in the area where a high deformation was expected; therefore, mesh distortion in the critical areas was not high during the forming simulation. The modeled specimen corresponds to the geometrical dimensions of the sheet samples used in the LDH testing according to ASTM E 2218-02 standard. Due to the symmetry conditions, a quarter of volume of the tooling and specimen was used in order to reduce the total number of nodes and elements, and thus to accelerate the calculations. Figure 6 shows the FE models of punch and sheet metal specimens with a trimming radius of 65 mm. The friction behavior was defined using an isotropic coulomb friction model with a uniform friction coefficient of 0.15. All contact behaviors between tooling and specimens were defined as surface to surface contact with finite sliding formulation, by which separation and sliding of the surfaces may rise a little. In the simulations, a blank holder force of 30 kN was applied to the sheet specimens. The forming limit diagram, the maximum φ_1 and minimum φ_2 strain values, as well as flow curves from the tensile test of the investigated steel SPCE 270, as presented in Figure 7, and anisotropy values r_0 , r_{45} , and r_{90} were used as input data for defining material properties in the FE simulations. Both isotropic and anisotropic simulations were performed. In case of the anisotropic simulation, the anisotropy values were converted to the anisotropic yield stress ratio of the Hill's yield criterion. This study aimed at comparing results of the forming limit curves calculated by different yield functions with regard to the anisotropy behaviour of the material.

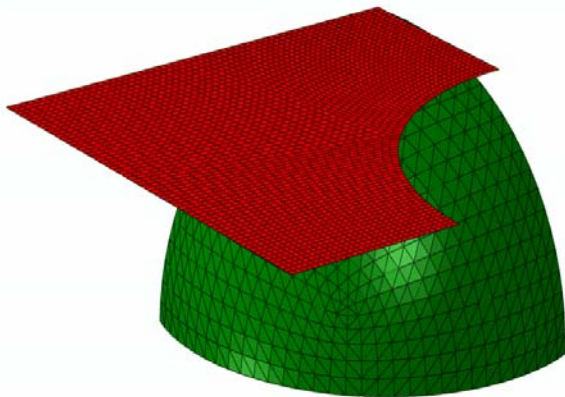


Figure 6. A quarter model of punch and specimen used in FEM simulation for the FLSD determination.

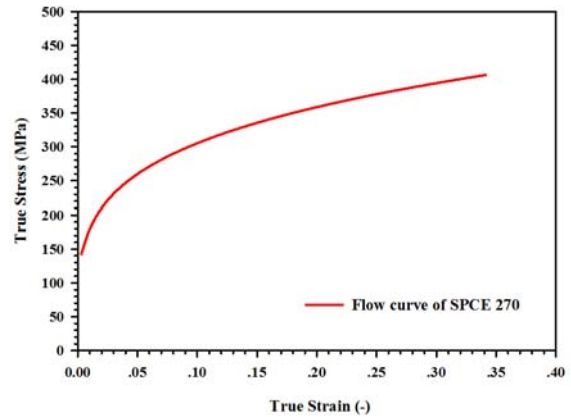


Figure 7. Flow curve of SPCE 270 steel sheet.

The method for determining forming limit stress curve by FE simulation is explained in detail as follows. The forming limit curve was initially determined by the LDH testing as described in the previous chapter. In this experiment, a constant forming velocity was kept and strain path was varied by the application of sheet specimens having a different trimmed radius. Afterwards, the LDH testing was simulated and the experimental FLC data were applied as a strain based failure criterion. At the point of time when the first critical elements of the sample reach the strain value defined by the FLC criterion in the simulation, necking is assumed to occur. At this moment, maximum and minimum in-plane stresses of these elements were taken and considered as the major and minor stresses for constructing one axis of the FLSC.

For the investigations in this study steel sheet of SPCE 270 grade was selected, as it is used for the examined part. The chemical composition of this low carbon steel and its mechanical properties determined by tensile test at room temperature are shown in Tables 1 and 2, respectively. The FLSD calculated by simulations coupled and uncoupled with Hill48 anisotropic yield stress ratio are demonstrated in Figures 8 and 9, respectively. Both forming limit stress curves are compared in Figure 10 to see their difference. The FLSC calculated by the anisotropic yield criterion exhibited better distributed stress values with higher magnitude than the isotropic criterion.

Table 1. Chemical composition of SPCE 270 Steel sheet, mass content in % ⁽¹⁴⁾.

SPCE 270	C	Si	Mn	P	S	Cr	Mo	Ni	Al	Ar	Co
	0.0024	0.0039	0.1342	0.0104	0.0067	0.0261	0.0022	0.0174	0	0.0512	0.0033
	Cu	Nb	Ti	V	W	Pb	Sn	B	Zn	N	Fe
0.0371	0.0017	0.0500	0.0023	<0.0010	0.0020	0.0035	0.0008	0.0012	0.0008	99.6400	

Table 2. Mechanical properties of SPCE steel sheet ⁽¹⁴⁾.

SPCE 270	Thickness	Yield Stress	Strength Coefficient	Strain Hardening Index	Anisotropy Rolling Direction	Anisotropy 45 degree Direction	Anisotropy transverse
	(mm)	σ_y (Mpa)	K (Mpa)	n	r_0	r_{45}	r_{90}
	0.8	142.37	521.2	0.2323	2.598	2.062	3.197

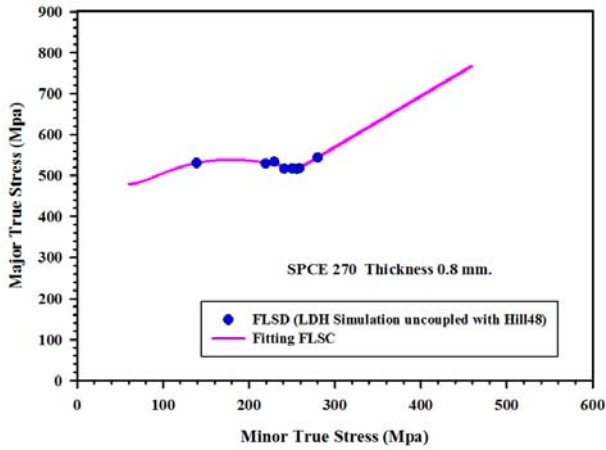


Figure 8. Determined forming limit stress diagram (FLSD) uncoupled with Hill48’s yield criterion (isotropic condition).

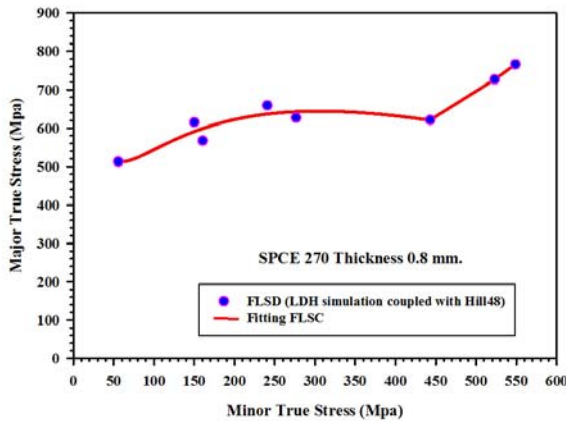


Figure 9. Determined forming limit stress diagram (FLSD) coupled with Hill48’s yield criterion (anisotropic condition).

The σ_1 axis corresponds to the uniaxial state of stress in tensile test, at which the minimum principal stress σ_2 is close to 0 MPa. For this condition, the maximum principal stress at failure was determined by FE simulation of the tensile test for the investigated material. Figure 10 illustrates that the FLSC of SPCE 270 steel sheet under consideration of material anisotropy behaviour according to the Hill48 yield criterion provided a definitely higher forming limit stresses than the FLSC without taking into account the anisotropy.

Whether the FLSC determined by using Hill48 yield criterion can more accurately predict material formability than the isotropic yield criterion will be checked in the following chapter.

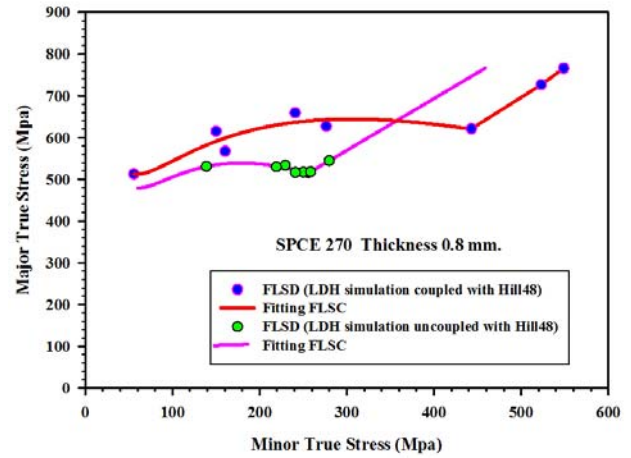


Figure 10. Comparison between the FLSDs calculated by simulations coupled and uncoupled with Hill 48’s yield criterion.

The stress based failure criterion FLSD can be used as an engineering tool for predicting the onset of necking during numerical simulation of any metal forming process. The principal stress state (σ_1, σ_2) of every FE element can be obtained for every step time by FE simulation. If all of the stress points (σ_1, σ_2) of a deformed part are located under the limit stress curve, there is no risk of failure and necking. If an element point of the part reaches or exceeds the limit curve, however, failure will occur in the area of that element and at the respective time step.

Application

In order to demonstrate the advantage of the FLSD criterion, an industrial automotive part was taken. Both experimental and FE numerical forming processes were carried out to form the part. The forming test was continued up to failure initiation. The industrial part was simulated by FEM in order to evaluate stress and strain values in the crack-critical area at the moment when the failure was observed in the experiment. The FLD and FLSD failure criterion could be verified by comparing the numerical and experimental results.

Figures 11, 12 and 13 illustrate the verification results for the industrial part. In Figure 11, the FLD of the investigated SPCE 270 steel as well as the maximum and minimum in-plane strains at the

crack initiation state for all elements of the part calculated by FE simulation are presented together in a strain diagram. Here, it can be observed that the calculated strain values of the part at the moment of failure lie far below the FLD curve. Thus, it was shown that the industrial part could be deformed up to this shape condition without unacceptable necking or failure. In fact, the part was already failed before this state in the experiment.

On the other hand, Figure 12 shows the FLSD calculated by FE simulation of the LDH testing uncoupled with Hill48 yield criterion and using the FLD data as failure criterion in comparison with the maximum and minimum in-plane stress values at the crack initiation state of the industrial part. These stresses locate closer to the determined FLSC, but some values still exceed the limit curve. The comparison between the FLSD calculated by simulation coupled with Hill48 anisotropic criterion and the in-plane stresses at the state of failure is illustrated in Figure 13. In this case, the stress values lie perfectly below the FLSC and the failure prediction by the FLSD is more precise. It is obvious that calculation using the Hill48 yield criterion led to an increase in accuracy of formability prediction. Finally, this work has confirmed that the FLSD can be used as an effective failure prediction tool. The FLSD indicated failure of the industrial part made of SPCE 270 steel with a thickness 0.8 mm after forming that is identical to the experiment. Nevertheless, at the same deformation state the FLD predicted a formed part without failure. This means that the FLSD calculated by the anisotropic model can provide a more precise forming limit prediction than the FLD.

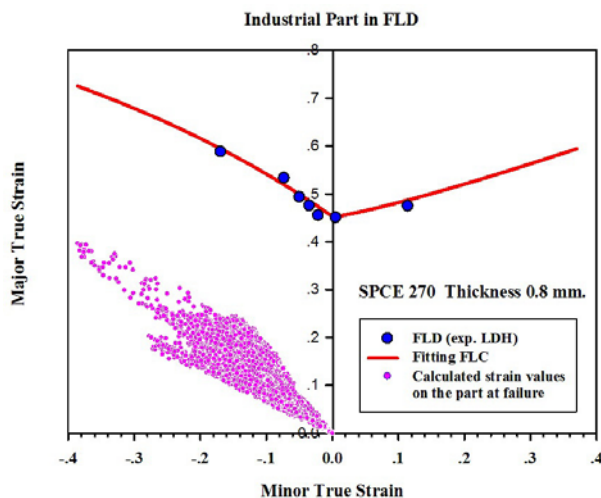


Figure 11. Verification of the FLD criterion with an industrial part made of SPCE 270.

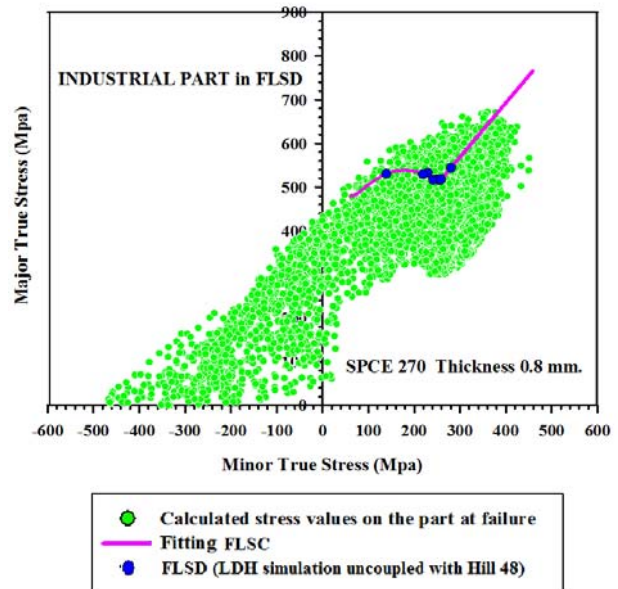


Figure 12. Verification of the FLSD criterion uncoupled with Hill48's yield criterion (isotropic condition) with an industrial part made of SPCE 270.

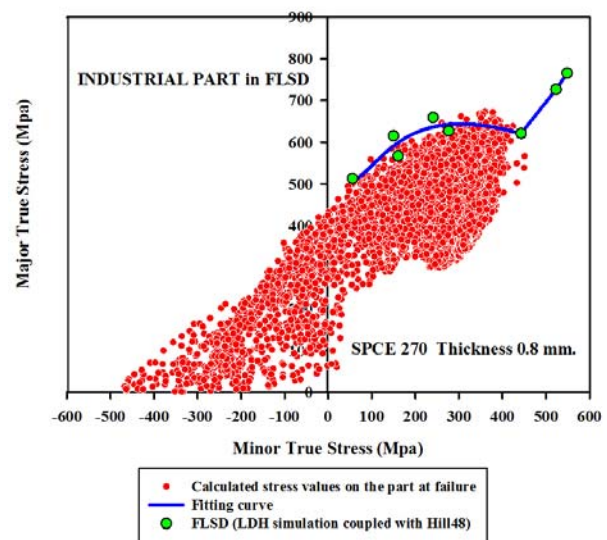


Figure 13. Verification of the FLSD criterion coupled with Hill48's yield criterion (anisotropic condition) with an industrial part made of SPCE 270.

Conclusions

A determination method of the stress based failure criterion for sheet metal forming was introduced. To obtain the FLSD FE simulations of the limit dome height testing were performed and maximum and minimum in-plane stresses for the critical area of tested samples were evaluated. The FLSD criterion was verified by an automotive part

made from mild steel sheet SPCE270. It was confirmed that the conventional forming limit diagram FLD is insufficient for predicting material failure in forming processes with accuracy, whereas the forming limit stress diagram FLSD can reveal formability limit of material more precisely. Additionally, the FLSD calculated by FE simulations coupled with Hill48 anisotropic yield criterion provides a better prediction than FE simulations using isotropic model. By applying the FLD and FLSD criterion to the pressed automotive part it was observed that the stress based failure criterion FLSD can reproduce the local state at crack initiation more realistically than the strain based failure criterion FLD. The accuracy of the FLSD depends strongly on the yield function applied in the calculation.

Acknowledgements

The authors would like to express their great thanks to the National Metal and Materials Technology Center (MTEC) for its excellent support of the limit dome height testing and tensile testing for the investigated steel.

References

1. Arrieux, R., Bedrin, C. & Boivin, M. (1982). Determination of an intrinsic forming limit stress diagram for isotropic sheets. In: *Proceedings of the 12th Biennial Congress of the International Deep Drawing Research Group*, Santa Margherita Ligure, Italy. **2**: 61-71.
2. Arrieux, R., Boivin, M. & Le Maître, F. (1987). Determination of the forming limit stress curve for anisotropic sheets. *CIRP Ann.-Manuf. Techn.* **36(1)**: 195-198.
3. Arrieux, R. (1997). Determination and use of the forming limit stress surface of orthotropic sheets. *J. Mater. Process. Tech.* **64(1-3)**: 25-32.
4. ASTM E 2218-02. (2002). Standard test method for determining forming limit curves: 1252-1266.
5. Buakaew, V., Sodamuk, S., Sirivedin, S. & Jirathearanat, S. (2007). Formability prediction of automotive parts using forming limit diagrams. *Journal of Solid Mechanics and Materials Engineering*. **1(5)**: 691-698.
6. Butuc, M.C., Gracio, J.J. & Barata da Rocha, A. (2003). A theoretical study on forming limit diagrams prediction. *J. Mater. Process. Tech.* **142(3)**: 714-724.
7. Butuc, M.C., Gracio, J.J. & Barata da Rocha, A. (2006). An experimental and theoretical analysis on the application of stress-based forming limit criterion. *Int. J. Mech. Sci.* **48(4)**: 414-429.
8. Hasek, V. (1973). Ueber den Formaenderungs- und Spannungszustand beim Ziehen von großen unregelmäßigen Blechteilen. *Berichte aus dem Institut fuer Umformtechnik*, University Stuttgart. 25: Verlag W. Girardet: Essen.
9. Kikuma, T. & Nakazima, K. (1971). Effects of deforming conditions and mechanical properties on the stretch forming limits of steel sheets. In: *Proceeding of ICSTIS*. **11**: 827-831.
10. Kobayashi, T., Ishigaki, H. & Abe, T. (1972). Sheet metal forming and formability. In: *Proceedings of the 7th Biennial Congress of the International Deep Drawing Research Group*, Amsterdam: 8.1-8.4.
11. Mueschenborn, W. & Sonne, H.M. (1975). *Archiv fuer das Eisenhuettenwesen* **46(9)**: 597-602.
12. Nakazima, K., Kikuma, T. & Hasuka, K. (1971). Study on the formability of steel sheets. *Yawata Technology Report* **284**: 678-680.
13. Nguyen Nhat, T. & Arrieux, R. (1995). Off-axes forming-limit stress diagrams of an anisotropic steel sheet. *J. Mater. Process. Tech.* **54(1-4)**: 193-198.
14. Sodamuk, S. (2007). *Formability prediction of automotive parts using forming limit diagrams*. Master Thesis in Mechanical Engineering. Srinakharinwirot University: 164.
15. Stoughton, T. B. (2000). A general forming limit criterion for sheet metal forming. *Int. J. Mech. Sci.* **42(1)**: 1-27.

16. Stoughton, T. B. (2001). Stress-based forming limits in sheet metal forming. *J. Eng. Mater. Technol.* **123(4)**: 417-422.
17. Stoughton, T. & Zhu, X. (2004). Review of theoretical models of the strain-based FLD and their relevance to the stress-based FLD. *Int. J. Plasticity* **20(8-9)**: 1463-1486.
18. Uthaisangsuk, V., Prah, U. & Bleck, W. (2007). Stress based failure criterion for formability characterisation of metastable steels. *Comp. Mater. Sci.* **39(1)**: 43-48.
19. Uthaisangsuk, V., Prah, U., Münstermann, S. & Bleck, W. (2008). Experimental and numerical failure criterion for formability prediction in sheet metal forming. *Comp. Mater. Sci.* **43(1)**: 43-50.
20. Uthaisangsuk, V. (2009). *Microstructure based formability modeling of multiphase steels*. Ph.D Thesis. RWTH Aachen University: 175.
21. Veerman, C. (1971). Sheet Metal Industries **48**: 678-690.